Proceedings of the
Annual Stability Conference
Structural Stability Research Council
Baltimore, Maryland, April 10-13, 2018

Improved Characterization of the Flexural and Axial Compressive Resistance of Noncomposite Longitudinally Stiffened Welded Steel Box-Section Members

Ajinkya M. Lokhande[1], Donald W. White[2], Charles M. King[3], Michael A. Grubb[4]

Abstract
There exists great potential for improvement of existing methods for calculating the flexural and axial compressive resistance of longitudinally stiffened welded steel box-section members, to achieve gains in the accuracy of their representation of the limit states responses as well as greater generality and ease of their design application. A good quantification of the ultimate compressive resistance of longitudinally stiffened plates is crucial for accurate characterization of the flexural and axial compressive resistance of these member types. This paper summarizes the conceptual and theoretical development of new methods for characterization of the ultimate compressive resistance of longitudinally stiffened plates, and the flexural and axial compressive resistance of longitudinally stiffened welded box-section members. The proposed method for calculating the plate compressive resistance is derived using an orthotropic plate idealization, but is expressed as a designer-friendly, intuitive column on elastic foundation model. This model considers the contributions from longitudinal stiffener flexure, transverse plate bending, and plate torsion. The proposed method for calculating member flexural resistance recognizes the inability of longitudinally stiffened flange plates to sustain large inelastic compressive strains beyond their maximum resistance, and therefore limits the flexural resistance of box sections with a longitudinally stiffened compression flange to the first yield of the compression flange in the effective cross-section. For sections involving early yielding of the tension flange, the member response is addressed rigorously via the direct calculation of the yield moment to the compression flange, considering the early yielding on the tension side of the neutral axis, and considering hybrid web, slender web and unstiffened slender or longitudinally stiffened compression flange effects as applicable. The paper presents a parametric study of longitudinally stiffened welded box columns whose failure mode involves combined flexural and local buckling, for which there is no experimental or finite element simulation data in the literature. The predictions using the proposed methods correlate well with the results from finite element test simulations, and with data compiled from experimental tests.

1. Introduction
Noncomposite steel box-section members are highly efficient in resisting loads and are used in various important areas of highway bridge construction as well as in building construction. The applications include but are not necessarily limited to truss members, arch ribs and ties, rigid-

[1] Graduate Research Assistant, Georgia Institute of Technology, <alokhande3@gatech.edu>
[2] Professor, Georgia Institute of Technology, <dwhite@ce.gatech.edu>
[3] Senior Steel Specialist, COWI Bridge, <cmk@cowi.com>
[4] Consultant, M.A. Grubb and Associates, LLC, <mgrubb@zoominternet.net>

frame members, columns, edge girders, floor beams and steel tower legs (see Fig. 1). For many of these types of components, longitudinal stiffening can provide material savings that justify the additional fabrication cost. For these types of members in larger bridges, longitudinal stiffening is essential to realization of the design. There is great potential for improvement of existing methods for design of these members to achieve gains in the accuracy of their representation of the limit states response as well as greater generality and ease of their design application.

Figure: 1 Longitudinally stiffened box-section member applications (Chou 2011 and GSG 2013)

Section 2 of this paper discusses a method for improved quantification of the ultimate compressive resistance of longitudinally stiffened plates. Section 3 discusses an improved calculation of the axial compressive resistance of longitudinally stiffened welded box-section members. Section 4 discusses new methods for characterization of the flexural resistance of longitudinally stiffened welded box-section members. Section 5 provides summary and concluding remarks.

2. Ultimate compressive strength of longitudinally stiffened plates

A good prediction of the ultimate compressive resistance of longitudinally stiffened plates is crucial for obtaining accurate characterization of the axial compressive and flexural resistance of longitudinally stiffened welded steel box-section members. Section 2.1 explains the need for the proposed method. Sections 2.2 and 2.3 explain the proposed method and its salient features. Section 2.4 discusses the evaluation of the performance of the proposed method.

2.1 Motivation

The prediction of the compressive resistance of longitudinally stiffened plates involves two steps: 1) Calculating the buckling strength, 2) Calculating the ultimate compressive strength. Table 1 provides a broad summary of the approaches for these two steps in existing methods.

The Eurocode (CEN 2006) and AISI (2016) effective width procedures use different combinations and forms of the methods listed in Table 1. The limitations of the approaches in AASHTO (2017) Article 6.11.8.2, Eurocode (CEN 2006) and AISI (2016) are discussed in detail in Lokhande (2018). They are summarized below, to explain the need for the proposed method.

<u>AASHTO (2017) Article 6.11.8.2</u>

The AASHTO (2017) method for calculating the ultimate compressive strength of longitudinally stiffened plates has the following shortcomings:

1) For slender plate subpanels susceptible to local buckling, the strength is limited to elastic buckling of the subpanel between the longitudinal stiffeners. This neglects the significant postbuckling resistance of the longitudinally stiffened plate subpanels.

2) The longitudinal stiffeners in wide plates with more than two longitudinal stiffeners tend to behave as unconnected struts. The key property influencing the compressive resistance of these types of plates is the moment of inertia of their longitudinal stiffeners. However, as pointed out

by King (2017), for these types of plates, the plate buckling coefficient in AASHTO, and hence the stiffened plate resistance, is expressed independently from this key property.

Table 1: Summary of existing methods for calculating the buckling and ultimate compressive resistances of longitudinally stiffened plates

Buckling resistance	**Ultimate compressive resistance**
1) Strut idealization: The strut model is based on treating a longitudinally stiffened plate as a series of separate columns comprised of the longitudinal stiffener and an associated width of the plate.	**1) Column strength curve:** Mapping to a column strength curve results in no consideration of the plate postbuckling resistance. Column strength curves have a short plateau (see Fig. 2).
2) Column on elastic foundation (CEF) idealization: The CEF model considers a longitudinal stiffener strut (i.e., the longitudinal stiffener and an associated width of the plate) resting on an elastic foundation representing the transverse bending stiffness of the plate. Thus it avoids the limitation of the strut idealization of neglecting the transverse bending stiffness of the plate. This can be significant especially in relatively narrow plates with one or two longitudinal stiffeners, which are commonly used in North America.	**2) Plate strength curve:** Mapping to a plate strength curve, e.g. Winter's curve, results in a consideration of the plate postbuckling resistance. Plate strength curves have a longer plateau (see Fig. 2). **3) Interpolation between column and plate strength curves:** Because of the lack of an explicit compressive strength curve for longitudinally stiffened plates, the Eurocode (CEN 2006) requires an interpolation between column and plate ultimate strength curves. Figure 2 clearly shows the higher compressive resistance for plates, due to postbuckling, and also the longer plateau for plate ultimate strengths compared to column strengths.
3) Orthotropic plate idealization: The orthotropic plate idealization smears the stiffness characteristics of the longitudinal stiffeners over the entire plate. Thus, it takes into account the longitudinal bending, transverse bending, and torsional stiffness of the plate.	

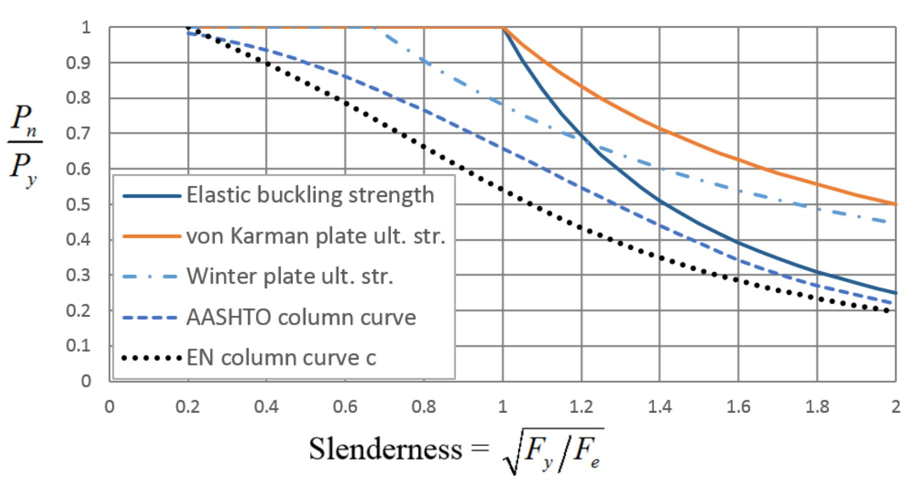

Figure 2: Axial compressive strength curves

3) For plates with more than two longitudinal stiffeners, AASHTO suggests the use of transverse stiffeners and requires the longitudinal stiffeners to satisfy a minimum moment of inertia requirement. This limits the designer's options in seeking the greatest design economy.
4) AASHTO (2017) requires a spacing of transverse flange stiffeners less than three times the width of the stiffened plate for the stiffeners to be considered effective. It would be better to provide design engineers more flexibility in choosing the transverse stiffener spacing.
5) AASHTO (2017) does not recognize the larger resistance of subpanels adjacent to the plate longitudinal edges.
6) AASHTO (2017) does not provide any guidance to prevent torsional buckling of tee and angle section stiffeners about the edge attached to the plate, i.e., "tripping" of the stiffeners.

AISI (2016)
The AISI (2016) effective width method for calculating the ultimate compressive strength of longitudinally stiffened plates has the following drawbacks:
1) The method is intended for plates containing formed stiffeners. It does not have any provisions addressing stiffener local buckling.
2) The buckling coefficient is calculated as the minimum of the coefficients for buckling of the plate between longitudinal stiffeners and overall buckling of the plate along with the longitudinal stiffeners. Thus it does not account directly for any interaction between local buckling of subpanels and overall buckling of the plate involving transverse displacement of the stiffeners.
3) The ultimate compressive strength of the stiffened plate is calculated by considering its postbuckling resistance using a form of Winter's effective width equation for unstiffened plates. It is inappropriate to count on this postbuckling resistance in all cases. For example, in a wide thin plate with a large number of longitudinal stiffeners, the longitudinal stiffeners and the tributary widths of the plate tend to behave as unconnected stiffener struts, i.e., as columns.

Eurocode (CEN 2006)
The Eurocode (CEN 2006) method for calculating the ultimate compressive strength of longitudinally stiffened plates has the following limitations:
1) Because of the lack of availability of an ultimate compressive strength curve for stiffened plates, it interpolates between a column strength curve (no postbuckling resistance and a short plateau length) and a nonlongitudinally stiffened plate strength curve (consideration of postbuckling resistance and a longer plateau length). As pointed out by King (2017), this interpolation can produce illogical results for slenderness values where the elastic buckling stress as a column approaches the elastic buckling stress as a plate. Furthermore, the calculations associated with this interpolation approach are relatively long and cumbersome.
2) It accounts for larger resistance of the half-width of the edge subpanels closest to the edge supports by considering that they reach the yield stress. However, as discussed later in this paper and in detail in Lokhande (2018), the maximum resistance of the stiffened plate typically occurs before the half-width of the subpanel closest to the edge support reaches the yield stress.

Hence, there is a need for a procedure that avoids the shortcomings of the existing methods.

2.2 Proposed method
The proposed method is based on the developments by King (2017). Sections 2.2.1 and 2.2.2 explain the calculation of the buckling and ultimate compressive resistance for longitudinally stiffened plates with equally-spaced and equal-size longitudinal stiffeners. Section 2.2.3 explains restrictions on the longitudinal stiffeners to prevent local buckling and tripping of the stiffeners.

2.2.1 Buckling resistance

The proposed method is based on an orthotropic plate idealization. Thus it considers all three contributions to the buckling resistance - longitudinal bending stiffness, transverse bending stiffness, and torsional stiffness. The differential equation of equilibrium for an orthotropic plate simply supported on all four edges and subjected to uniform longitudinal compression is

$$D_x \frac{\partial^4 \delta}{\partial x^4} + 2H \frac{\partial^4 \delta}{\partial x^2 \partial y^2} + D_y \frac{\partial^4 \delta}{\partial y^4} = -\frac{P_x}{b_{sp}} \frac{\partial^2 \delta}{\partial x^2} \tag{1}$$

where:

x is the longitudinal direction of the plate;

y is the width direction of the plate;

δ is the transverse displacement of the plate;

$$D_x = EI_s / w \tag{2}$$

= flexural stiffness for bending about the y axis, where I_s is the moment of inertia of an individual stiffener strut composed of the stiffener plus the tributary width of the longitudinally stiffened plate, *w*, taken about an axis parallel to the face of the plate and passing through the centroid of the gross area of the stiffener strut;

$$H = \frac{Et_{sp}{}^3}{12\left(1-\nu^2\right)} = \text{torsional stiffness} \tag{3}$$

$$D_y = \frac{Et_{sp}{}^3}{12\left(1-\nu^2\right)} = EI_p = \text{flexural stiffness for plate bending about the x axis} \tag{4}$$

P_x is the elastic buckling load of the longitudinally stiffened plate;

E is the modulus of elasticity; and

Figure 3 illustrates the dimensional and area variables employed above and in the subsequent discussions for a representative longitudinally stiffened plate.

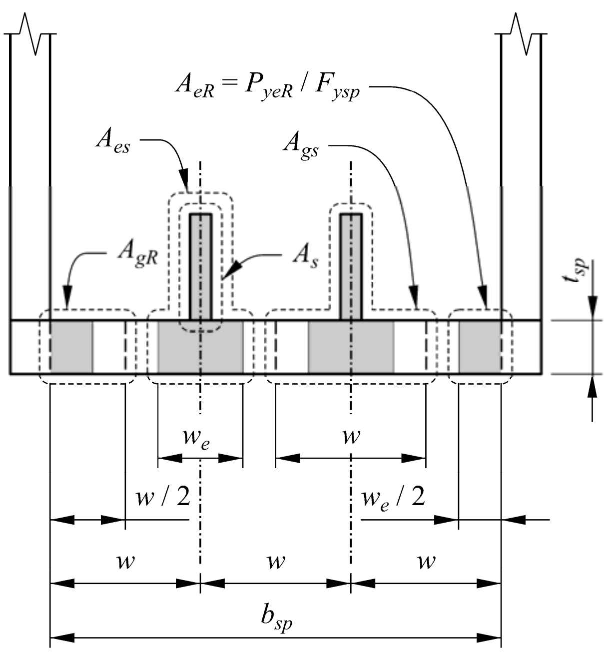

Figure 3: Illustration of variables for a longitudinally stiffened plate

Assuming the buckling mode of the stiffened plate is the same as that of an unstiffened plate of overall width b_{sp} between simply-supported edges,

$$\delta = \delta_{\max} \sin\frac{m\pi x}{\ell}\sin\frac{q\pi y}{b_{sp}} = eS_a S_b \tag{5}$$

where ℓ is the buckling length, taken as the smaller of the transverse stiffener spacing, *a*, and the characteristic buckling length, ℓ_c, explained below. Substituting this displacement solution, which satisfies Eq. (1) and the specified boundary conditions, one can write:

$$\frac{P_x}{b_{sp}} e\left(\frac{m\pi}{\ell}\right)^2 S_a S_b = D_x e\left(\frac{m\pi}{\ell}\right)^4 S_a S_b + 2He\left(\frac{m\pi}{\ell}\right)^2\left(\frac{q\pi}{b_{sp}}\right)^2 S_a S_b + D_y e\left(\frac{q\pi}{b_{sp}}\right)^4 S_a S_b \tag{6}$$

Taking $m = 1$ and $q = 1$,

$$\frac{P_x}{b_{sp}}\left(\frac{\pi}{\ell}\right)^2 = \frac{EI_s}{w}\left(\frac{\pi}{\ell}\right)^4 + 2EI_p\left(\frac{\pi}{\ell}\right)^2\left(\frac{\pi}{b_{sp}}\right)^2 + EI_p\left(\frac{\pi}{b_{sp}}\right)^4 \tag{7}$$

Since

$$b_{sp} = (n+1)w \tag{8}$$

where *n* is the number of longitudinal stiffeners, the elastic buckling load of the longitudinally stiffened plate may be expressed as

$$P_x = (n+1)EI_s\left(\frac{\pi}{\ell}\right)^2 + 2b_{sp}EI_p\left(\frac{\pi}{b_{sp}}\right)^2 + b_{sp}EI_p\left(\frac{\pi}{b_{sp}}\right)^4\left(\frac{\ell}{\pi}\right)^2 \tag{9}$$

This buckling load also can be conveyed as an intuitive and easy-to-use column on elastic foundation model, as explained below.

The buckling load per stiffener may be expressed as

$$\frac{P_x}{(n+1)} = EI_s\left(\frac{\pi}{\ell}\right)^2 + 2\frac{1}{(n+1)}b_{sp}EI_p\left(\frac{\pi}{b_{sp}}\right)^2 + b_{sp}\frac{1}{(n+1)}EI_p\left(\frac{\pi}{b_{sp}}\right)^4\left(\frac{\ell}{\pi}\right)^2 \tag{10}$$

$$\frac{P_x}{(n+1)} = \left[EI_s\frac{\pi^2}{\ell^2} + \pi^4 w\frac{EI_p}{b_{sp}^4}\frac{\ell^2}{\pi^2}\right] + \frac{\pi^2}{3(n+1)(1-\nu)}\frac{Gt_{sp}{}^3}{b_{sp}} \tag{11}$$

$$\frac{P_x}{(n+1)} = P_{es} = P_{esF} + P_{esT} \tag{12}$$

where:

$P_{esF} = \left[\dfrac{\pi^2 EI_s}{\ell^2} + k_p\dfrac{\ell^2}{\pi^2}\right]$ = elastic flexural buckling resistance of an individual stiffener strut (13)

$P_{esT} = \dfrac{\pi^2}{(1-\nu)b_{sp}^2}\dfrac{Gwt_{sp}^3}{3}$ = plate torsional stiffness contribution to the buckling resistance of each stiffener strut (14)

$k_p = \pi^4 w\dfrac{EI_p}{b_{sp}^4}$ = plate lateral stiffness coefficient (15)

For an infinitely long plate the characteristic buckling length, ℓ_c, is the length that results in the minimum value of P_{es}. Therefore, $\frac{dP_{es}}{d\ell_c} = \frac{d\left(\frac{\pi^2 EI_s}{\ell_c^{\,2}} + k_p \frac{\ell_c^{\,2}}{\pi^2}\right)}{d\ell_c} = 0$ gives

$$\ell_c = \left(\frac{EI_s\pi^4}{k_p}\right)^{1/4} \tag{16}$$

2.2.2 Ultimate compressive resistance

Knowing the elastic buckling load $P_{es} = P_{esF} + P_{esT}$, the ultimate compressive strength of a longitudinally stiffened plate with equally spaced and equal size stiffeners can be calculated as

$$P_{nsp} = \sum P_{ns} + 2P_{nR} \tag{17}$$

where:

$P_{ns} = P_{nsF} + 0.15P_{esT} \le P_{yes}$ = nominal compressive resistance of an individual stiffener strut composed of the stiffener plus the tributary width of the longitudinally stiffened plate (18)

P_{nsF} = nominal flexural buckling resistance of an individual stiffener strut determined by mapping the elastic flexural buckling load P_{esF} to the AASHTO column curve as shown below:

If $\frac{P_{ys}}{P_{esF}} \le 2.25$, then

$$P_{nsF} = 0.658^{\frac{P_{ys}}{P_{esF}}} P_{yes} \tag{19}$$

Otherwise,

$$P_{nsF} = 0.877\frac{P_{esF}}{A_{gs}} A_{es} \tag{20}$$

$P_{nR} = \left(1 - \frac{P_{ns}}{P_{yes}}\right)\left(F_{ysp} + \frac{P_{ns}}{A_{es}}\right)0.45A_{gR} + \left(\frac{P_{ns}}{P_{yes}}\right)P_{yeR} \le P_{yeR}$ = compressive resistance provided by an individual laterally-restrained longitudinal edge of the longitudinally stiffened plate (21)

Equation 21 recognizes that the edge stress is larger than the ultimate stress of the stiffener strut and it also takes into account the observation by Lokhande (2018) and King (2017) that the edge stress is typically less than the yield stress at the ultimate strength condition. Equation 21 is a simple linear interpolation between (1) the yield load of the edge, P_{yeR}, based on the plate effective width tributary to the edge, in the limit that P_{ns} is equal to P_{yes}, and (2) the compression force given by a weighted average of F_{ysp} and the maximum compression stress on the adjacent stiffener strut, P_{ns}/A_{es}, acting on A_{gR}, in the limit that P_{ns} becomes small. Figure 4 shows the stress distribution and the corresponding effective width when P_{ns} is equal to P_{yes}, which corresponds to a plate local buckling mode. Figure 5 shows the stress distribution and the corresponding effective width when P_{ns} becomes small, which corresponds to an overall buckling mode.

$P_{yeR} = F_{ysp}\left(w_e/2\right)t_{sp}$ = effective yield load of an individual laterally-restrained longitudinal edge of the longitudinally stiffened plate (22)

$P_{yes} = F_{ysp}A_{es}$ = effective yield load of an individual stiffener strut (23)

$P_{yR} = F_{ysp}\left(w/2\right)t_{sp}$ = yield load of an individual laterally-restrained longitudinal edge of the longitudinally stiffened plate (24)

$P_{ys} = F_{ysp}A_{gs}$ = yield load of an individual stiffener strut (25)

$A_{es} = A_s + w_e t_{sp}$ = effective area of an individual stiffener strut (26)

$A_{gR} = \left(w/2\right)t_{sp}$ = gross area for the laterally-restrained longitudinal edge of the plate (27)

$A_{gS} = A_s + wt_{sp}$ = gross area of an individual stiffener strut (28)

A_s = gross area of an individual longitudinal stiffener, excluding the tributary width of the longitudinally stiffened plate;
F_{ysp} = specified minimum specified yield strength of the longitudinally stiffened plate;
w_e = effective width of the plate between the longitudinal stiffeners or between a longitudinal stiffener and the laterally-restrained longitudinal edge of the longitudinally stiffened plate, as applicable, calculated using the modified Winter's effective width equation given in Lokhande and White (2017) with F_{cr} taken as F_{ysp} and with λ_r taken as $1.09\sqrt{E/F_{ysp}}$ (in.)

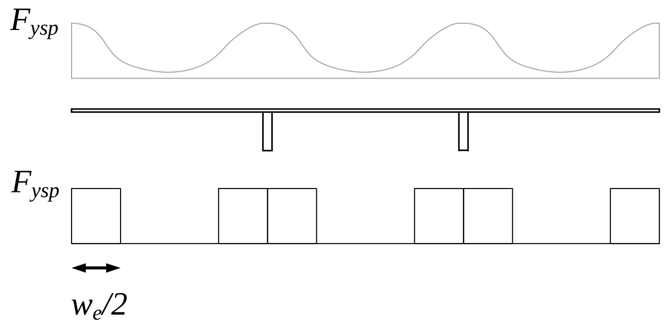

Figure 4: Stress distribution and the corresponding effective width when P_{ns} is equal to P_{yes}

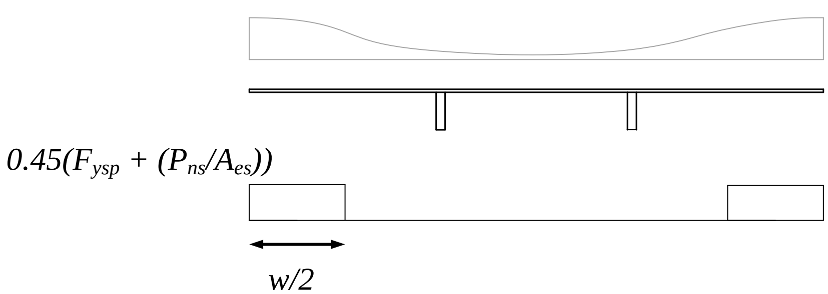

Figure 5: Stress distribution and the corresponding effective width when P_{ns} becomes small

2.2.3 Restrictions on the cross-section of the longitudinal stiffeners

The longitudinal stiffeners must satisfy the following requirements:

- The yield strength of the stiffeners shall not be less than the yield strength of the plate to which they are attached.
- The slenderness of the of the longitudinal stiffener cross-section elements is to be such that local buckling does not impact the resistance of the longitudinal stiffeners.

- Additionally, tee and angle section stiffeners must satisfy $\left(J_s/I_{ps}\right) \geq 5.0\left(F_{ysp}/E\right)$, which ensures that torsional buckling of these stiffeners about the edge of the stiffener attached to the plate is prevented. In this equation, J_s is the St. Venant torsional constant of the longitudinal stiffener alone, not including the contribution from the stiffened plate, and I_{ps} is the polar moment of inertia of the longitudinal stiffener alone about the attached edge. For flat plate stiffeners, this corresponds to a slenderness limit of $0.45\sqrt{E/F_y}$, which is the nonslender plate limit specified in AASHTO (2017) Article 6.9.4.2.1.

2.2.4 Extension to plates with unequally spaced/unequal size longitudinal stiffeners and transverse stiffener design

An extension of the proposed method to calculate the buckling resistance and ultimate compressive resistance of longitudinally stiffened plates with unequally spaced and/or unequal size longitudinal stiffeners is explained in White et al. (2018) and Lokhande (2018). In addition, guidelines for design of transverse stiffeners provided to enhance the compressive strength of longitudinally stiffened plates, are also explained in these references.

2.3 Salient features of the proposed method

The salient features of the proposed method are as follows:

1) It is derived using an orthotropic plate idealization and thus considers all three contributions to the buckling resistance - longitudinal bending, transverse bending, and torsional stiffness.

2) The buckling resistance obtained using the orthotropic plate idealization is expressed as an intuitive and easy-to-use column on elastic foundation model. The elastic torsional contribution from the plate is included directly in the ultimate strength calculation, with a calibrated reduction factor of 0.15. This results in a longer plateau than that for the compression member buckling curve. As pointed out by King (2017), the plate torsional stiffness provides much of the stability to plates with a buckling resistance close to the yield stress.

3) The explicit combination of the three contributions to the stiffened plate compressive resistance facilitates design optimization since the relative importance of each effect is clear.

4) The method is applicable to longitudinally stiffened plates with or without intermediate transverse stiffeners.

5) The characteristic buckling length concept is familiar to the engineer. This allows the engineer to make a good decision about whether transverse stiffening is needed, and at what spacing to place transverse stiffeners if they are used.

6) The method recognizes that the edge stress is larger than the ultimate stress of the stiffener struts, but it also takes into account the observation that the edge stress is typically less than the yield stress at the ultimate strength condition.

7) The method recognizes the postbuckling resistance of the plate panels between the longitudinal stiffeners, and/or between the longitudinal stiffeners and the laterally-restrained longitudinal edge of the stiffened plate.

8) Unlike Eurocode (CEN 2006), the method does not resort to an interpolation between column-type and plate-type curves to determine the extent of the plate-like behavior.

9) The method also provides guidance for calculating the compressive resistance of plates with unequally-spaced and/or unequal-size longitudinal stiffeners. These recommendations provide an accurate to conservative estimate of the compressive resistance for more general configurations.

10) The method does not recognize extensive postbuckling resistance of longitudinally stiffened plates with relatively weak longitudinal stiffener struts that fail at low values of the compression stress. These types of configurations are a quite inefficient use of the additional longitudinal stiffener material plus the fabrication cost in the context of welded box-section member construction. Therefore, this is not viewed as a limitation.

2.4 Evaluation of the performance of the proposed method

Four non-dimensional parameters influencing the compressive resistance of a longitudinally stiffened plate are identified, and they may be used to generate the geometries for parametric studies. The identification of these non-dimensional parameters is discussed below.

Based on Section 2.2, the buckling load of a longitudinal stiffener strut P_{es} may be expressed as

$$P_{es} = P_{esF} + P_{esT} = \left[EI_s \frac{\pi^2}{\ell^2} + k_p \frac{\ell^2}{\pi^2} \right] + \frac{\pi^2}{3(n+1)(1-\nu)} \frac{G t_{sp}^{\ 3}}{b_{sp}} \tag{29}$$

For an infinitely long plate, where $\ell = \ell_c$, P_{esF} may be written as

$$P_{esF} = \frac{2\pi^2}{b_{sp}^2} \frac{E t_{sp}^3}{12(1-\nu^2)} w \left(\sqrt{\frac{I_s}{w I_p}} \right) \tag{30}$$

and P_{esT} may be written as

$$P_{esT} = \frac{2\pi^2}{b_{sp}^2} \frac{E t_{sp}^3}{12(1-\nu^2)} w \tag{31}$$

Knowing $A_{gS} = A_s + w t_{sp}$, the corresponding stresses $F_{esF} = P_{esF} / A_{gS}$ and $F_{esT} = P_{esT} / A_{gS}$ can be written as

$$F_{esF} = \frac{\pi^2 E}{6(1-\nu^2)} \frac{1}{(n+1)^2} \frac{1}{\left(\dfrac{w}{t_{sp}} \right)^2} \frac{1}{\left(\dfrac{A_{gS}}{w t_{sp}} \right)} \left(\sqrt{\frac{I_s}{w I_p}} \right) \tag{32}$$

and

$$F_{esT} = \frac{\pi^2 E}{6(1-\nu^2)} \frac{1}{(n+1)^2} \frac{1}{\left(\dfrac{w}{t_{sp}} \right)^2} \frac{1}{\left(\dfrac{A_{gS}}{w t_{sp}} \right)} . \tag{33}$$

Therefore, it is apparent that four non-dimensional parameters n, $\dfrac{w}{t_{sp}}$, $\dfrac{A_{gS}}{w t_{sp}}$ and ℓ should be considered in parametric studies to evaluate the performance of the recommended calculations. It should be noted that both $A_{gS}/(w t_{sp})$ and $I_s/(w I_p)$ provide a measure of the contribution of the stiffener strut compared to the contribution from the associated plate width. The term $A_{gS}/(w t_{sp})$ is selected over $I_s/(w I_p)$ as it appears in both the F_{esF} and F_{esT} terms. Also, for F_{esF} the influence of $A_{gS}/(w t_{sp})$ is larger than $I_s/(w I_p)$ since $I_s/(w I_p)$ appears under the radical.

The performance of the proposed method using data compiled from experimental tests and FE test simulations is evaluated in Lokhande (2018). It is shown that the predictions using the proposed method correlate well with benchmark results, and are significantly better than the predictions using the methods in AASHTO (2017), AISI (2016), and Eurocode (CEN 2006).

3. Axial compressive resistance of longitudinally stiffened welded box-section members

As mentioned earlier, a good prediction of the ultimate compressive resistance of longitudinally stiffened plates is crucial for obtaining a more accurate characterization of the axial compressive resistance of longitudinally stiffened welded steel box-section members. Section 3.1 explains the proposed method for calculating the axial compressive resistance of longitudinally stiffened welded steel box-section members using the method in Section 2 for calculating the ultimate compressive resistance of longitudinally stiffened plates. At the present time (2018), there is no experimental or finite element simulation data in the literature quantifying the interaction between flexural and local buckling on the axial compressive resistance of longitudinally stiffened welded steel box-section members. Section 3.2 shows the performance of the proposed method using the results of a parametric study performed using FE simulations.

3.1 Proposed method

The axial compressive resistance P_n is given as follows:

$$P_n = F_{cr} A_{eff} \tag{34}$$

where:

$$A_{eff} = \sum_{nlsp} b_e t + \sum_{c} A_c + \sum_{lsp} \left(A_{eff} \right)_{sp} \tag{35}$$

in which the summations are over the nonlongitudinally stiffened plates, the corners of the box section, and the longitudinally stiffened plates;

b_e = effective width of the nonlongitudinally stiffened element under consideration, determined as specified in Article 6.9.4.2.2b of AASHTO (2017) (for non-slender nonlongitudinally stiffened plate elements, $b_e = b$);

t = thickness of the element under consideration;

A_c = gross cross-sectional area of the corner pieces of a box section;

$\left(A_{eff} \right)_{sp} = P_{nsp} / F_{ysp}$ = effective area of the longitudinally stiffened plate under consideration (36)

P_{nsp}= nominal compressive resistance of the longitudinally stiffened plate element under consideration, calculated using the proposed method in Section 2.

F_{cr} is the axial stress on the cross-section effective area at the member nominal compressive resistance, calculated as follows:

If $\frac{P_{os}}{P_e} \le 2.25$, then

$$F_{cr} = \left[0.658^{\frac{P_{os}}{P_e}} \right] F_y \tag{37}$$

Otherwise,

$$F_{cr} = 0.877 P_e / A_g \tag{38}$$

where:
A_g = total gross cross-sectional area of the member, including any longitudinal stiffeners;
P_e = member elastic buckling load based on the gross cross-sectional properties; and

$$P_{os} = \sum_{nlsp} F_y bt + \sum_{c} F_y A_c + \sum_{lsp} F_{ysp} \left(A_{eff} \right)_{sp} \tag{39}$$

Equation 34 captures the influence of the "local" strengths of the nonlongitudinally and longitudinally stiffened plates on the overall member axial compressive resistance.

3.2 Evaluation of the proposed method performance

The performance of the proposed method is evaluated below using the results from FE test simulations. Table 2 summarizes the parametric study design. Three non-dimensional parameters are investigated pertaining to the each of the flange and web plates. Also, the overall slenderness L/r_{min} is varied for these longitudinally stiffened box-section members.

Table 2: Summary of parametric study variables for evaluating the performance of the proposed calculation of the axial compressive resistance for longitudinally stiffened box section members

Case Numbers	**Flange plates**			**Web plates**			**Column**
	w/t_{sp}	n	A_{gS}/wt_{sp}	w/t_{sp}	n	A_{gS}/wt_{sp}	$L/r_{\min}$
1, 2, 3	20	1	1.1	20	2	1.1	50, 80, 110
4, 5, 6	20	1	1.1	20	2	1.4	50, 80, 110
7, 8, 9	20	1	1.1	60	1	1.1	50, 80, 110
10, 11, 12	20	1	1.1	60	1	1.4	50, 80, 110
13, 14, 15	20	1	1.1	60	2	1.1	50, 80, 110
16, 17, 18	20	1	1.1	60	2	1.4	50, 80, 110
19, 20, 21	20	2	1.1	60	1	1.1	50, 80, 110
22, 23, 24	20	2	1.1	60	1	1.4	50, 80, 110
25, 26, 27	20	2	1.1	60	2	1.1	50, 80, 110
28, 29, 30	20	2	1.1	60	2	1.4	50, 80, 110
31, 32, 33	60	1	1.1	60	2	1.1	50, 80, 110
34, 35, 36	60	1	1.1	60	2	1.4	50, 80, 110
37, 38, 39	60	1	1.4	60	2	1.1	50, 80, 110
40, 41, 42	60	1	1.4	60	2	1.4	50, 80, 110

The dimensions of the 42 box-section members are obtained by setting the thickness of the flanges and webs as one inch. A range of column slenderness values are considered to study the interaction between local and global buckling of the members. Slenderness values $L/r_{\min}$ of 50, 80 and 110 correspond to F_{cr} = $0.83F_y$, $0.63F_y$ and $0.41F_y$ respectively; where $F_y = 50$ ksi. Flat longitudinal stiffeners are used, and it is ensured that the slenderness of the stiffener plate does not exceed $0.48\sqrt{E/F_y}$ to prevent local buckling/tripping of the longitudinal stiffener. Details of the finite element models are explained in Lokhande (2018). Figure 6 shows a comparison of the member test simulation strength to the strengths predicted using the proposed method and using the corresponding procedures from AISI (2016) and the Eurocodes (CEN 2005 and 2006).

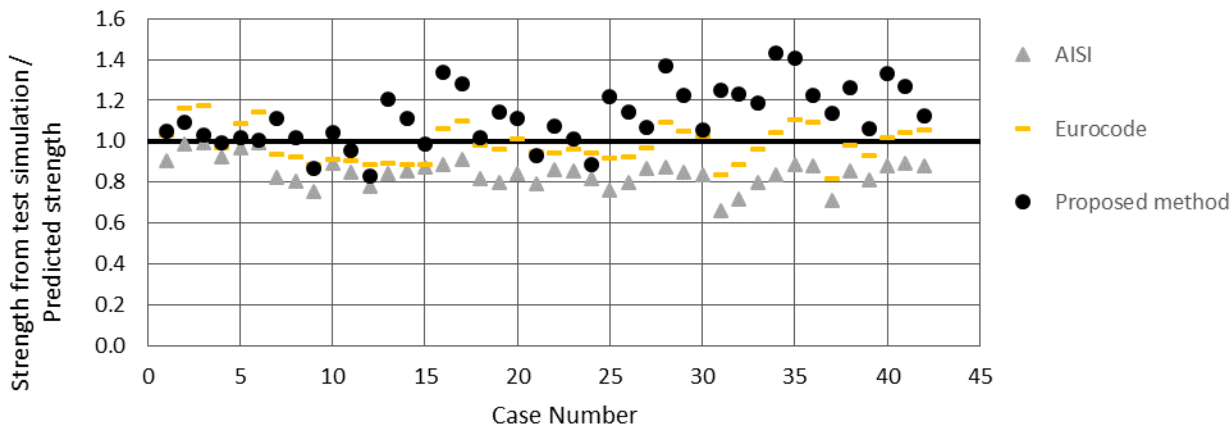

Figure 6: Comparison of the member strength from test simulation with the strength predcited using the proposed method

The reasons for the under- and over-prediction of the axial compressive resistances by the proposed method are as follows:

- It has been found that the plate resistance predictions using the method detailed in Section 2 vary from accurate to somewhat conservative as w/t_{sp} increases. There are two reasons for the under-prediction of the plate resistance when $w/t_{sp} = 60$:
  - o Conservatism of the modified form of Winter's effective width equation in Article 6.9.4.2.2b of AASHTO (2017) for large w/t_{sp} .
  - o The modified form of Winter's effective width equation in AASHTO (2017) does not account for the restraint from the adjacent subpanels between longitudinal stiffeners.

- For box section members with large w/t_{sp} and $L/r_{\min}$, the interaction between global flexural buckling of the member and local buckling of the component plates results in axial compressive resistances smaller than the predicted resistance. It can be observed that for Cases 1 to 6 in which all the plates have $w/t_{sp} = 20$ (theoretically no local buckling of the subpanels between longitudinal stiffeners) the proposed method gives an accurate to slightly conservative prediction. However, for cases in which $w/t_{sp} = 60$ and $L/r_{\min} = 110$ (e.g., Cases 9, 12, 21, 24) the strength is slightly lower than the predicted strength due to significant local-global buckling interaction.

- Studies are underway to investigate additional potential cases where local-global buckling interaction may cause the greatest unconservatism. These include cases with L/r_{min} up to 120, which is the maximum limit in the AASHTO LRFD Specifications for primary members, with w/t_{sp} up to 90, which is the maximum limit on the slenderness of longitudinally stiffened plate subpanels in the proposed provisions. It should be noted that for box columns subjected to significant axial compression, the maximum w/t_{sp} will commonly be limited to values closer to 40, since the recommended provisions disallow theoretical plate buckling under construction, service and fatigue loading conditions. Preliminary results indicate maximum unconservatism close to the values shown in Fig. 6.

Generally, large w/t_{sp} values will only be encountered in longitudinally stiffened box-section beams. These members may have a small axial force and hence an engineer may need to calculate the axial compressive resistance of these members with large w/t_{sp} values. However, in these members because P_u / P_n is small, the under-prediction of P_n will have a minor impact on the overall strength prediction for combined axial compression and bending.

- Figure 7 shows a comparison of the member test simulation strengths to the strengths predicted using the proposed method (using the AISC/AASHTO column curve), and the proposed method using the Eurocode column curve b. Figure 7 clearly shows that the un-conservatism of the strength prediction for columns with large L/r_{min}, as well as the dispersion in the resulting predictions, can be improved by using Eurocode column curve b instead of the more optimistic AISC/AASHTO column curve.

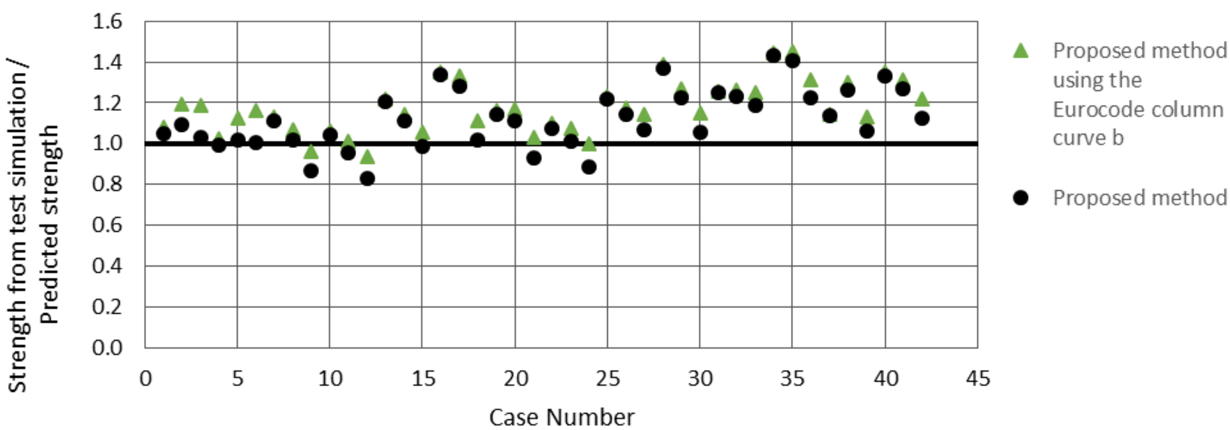

Figure 7: Comparison of the member test simulation strength to the strengths predicted using the proposed method using the AISC/AASHTO column curve, and the proposed method using the Eurocode column curve b

The unconservatism of the predictions using AISI (2016) and Eurocode (CEN 2006) methods (shown in Fig. 6) can be attributed to their optimistic prediction of the ultimate compressive resistance of longitudinally stiffened welded plates. This has been clearly shown in Lokhande (2018) where the ultimate compressive resistance of longitudinally stiffened welded plates obtained from FE simulations and experimental tests have been compared with the predictions using AISI (2016) and Eurocode (CEN 2006) methods. The drawbacks of the AISI (2016) and Eurocode (CEN 2006) methods for calculating the ultimate compressive resistance of longitudinally stiffened plates have been discussed in Section 2.1.

The accurate to conservative prediction of the resistance for cases 1, 4, 7, 10, 13, 16, 19, 22, 25, 28, 31, 34, 37, 40, which have $F_{cr} = 0.83F_y$ and have component plates with different ultimate stress capacity, shows that the proposed method works well even for cases involving significant force redistribution between relatively weak and relatively strong plate elements (One extreme example is Case 13, in which in the ultimate stress capacity of the web plate is 1/4th of the ultimate stress capacity of the flange plate).

4. Flexural resistance of longitudinally stiffened welded box-section members

With the goal of conceptual consistency with respect to the method for nonlongitudinally stiffened members recommended by Lokhande and White (2017), two methods for characterizing the flexural resistance of longitudinally stiffened box-section members are proposed. These are explained in detail in Section 4.2. Section 4.1 discusses the limitations of the existing methods for calculation of the flexural resistance of longitudinally stiffened welded steel box-section members and thus highlights the motivation for the proposed methods.

4.1 Limitations of existing methods

The AASHTO (2017) provisions do not address noncomposite box sections with longitudinal stiffening. The AASHTO (2017) provisions restrict the maximum flexural resistance of composite box girders to the yield moment of the compression or the tension flange. Similarly, the Eurocodes (CEN 2005; CEN 2006) limit the maximum flexural resistance of Class 4 sections to the yield moment of the effective elastic cross-section. However, based on the observations for nonlongitudinally stiffened box-section beams, there is significant reserve strength beyond the first yield of the tension flange. Section F2.4.1 of AISI (2016) allows the consideration of inelastic reserve strengths considering partial plastification, subject to certain restrictions including:

- The flexural resistance is not allowed to exceed 1.25 times the yield moment
- The ratio of the depth of the compressed portion of the webs to their thickness is not allowed to exceed $1.11\sqrt{E/F_y}$.

Based on the observations for nonlongitudinally stiffened box-section beams and also by considering that for nonlongitudinally stiffened webs the noncompact web limit λ_{rw} (Lokhande and White 2017) is more than two times the value of $1.11\sqrt{E/F_y}$, it appears that the AISI rules are too prohibitive and would result in a failure to consider larger available resistances in I-section members. In addition:

- AASHTO (2017) does not address the possibility of lateral torsional buckling.
- The Eurocode method requires an iterative or at least a two-step calculation for obtaining the effective cross-section for Class 4 sections.
- According to AISI (2016), the flexural resistance is calculated using effective section properties where the effective section is obtained using an effective width of the flanges and webs, using the provisions in Appendix 1 of AISI (2016). However, Appendix 1 does not specifically have provisions for longitudinally stiffened webs subjected to a stress gradient.

A good quantification of the ultimate compressive resistance of longitudinally stiffened plates is crucial for obtaining an accurate characterization of the flexural resistance of welded box-section members with a longitudinally stiffened compression flange. The limitations of the AASHTO, Eurocode and AISI approaches for calculation of the ultimate compressive resistance of a longitudinally stiffened plate have been discussed in Section 2. Therefore, clearly there is a need for a new method to obtain an improved quantification of the flexural resistance of these types of members.

4.2 Proposed methods

Two methods for characterizing the flexural resistance of longitudinally stiffened box-section members are proposed in this section:

Method 1, applicable to box-section members with a nonlongitudinally stiffened compression flange and longitudinally stiffened webs. The proposed method for characterizing the cross-section flexural resistance of these member types is the same as that for nonlongitudinally stiffened box-section members (Lokhande and White 2017) except the web load-shedding factor, R_b, should be calculated using the provisions recommended by Subramanian and White (2017) for longitudinally stiffened webs, using a_{wc} determined with $b_{fc}t_{fc}$ taken as $A_{eff}/2$, and D_c taken as D_{ce}, where A_{eff} is the effective area of the compression flange calculated using the modified Winter's equation given in Lokhande and White (2017). These provisions have been balloted and approved for the next release of the AASHTO LRFD Specification in 2020. The hybrid factor, R_h, should be calculated using AASHTO (2017) Eq. 6.10.1.10.1-1, but with A_{fn} taken as one-half of the effective flange area, $A_{eff}/2$.

Method 2, applicable to box cross-section members with a stiffened compression flange. There are two main differences between the proposed method for characterizing the flexural resistance of longitudinally stiffened box-section members with a stiffened compression flange and the method recommended by Lokhande and White (2017) for characterizing the flexural resistance of nonlongitudinally stiffened box-section members:

1) Effective cross-section: Unlike box sections with a nonlongitudinally stiffened compression flange, the effective cross-section of a box section with a longitudinally stiffened compression flange is as shown in Fig. 8, where:

$$A_{eff.p2} = P_{nsp}/F_{ysp} \tag{40}$$

P_{nsp} = ultimate compressive resistance of the longitudinally stiffened flange determined using the proposed method in Section 2.

c = the distance of the centroid of the gross area of the flange plate and its longitudinal stiffeners from the top of the web plates. AISI (2016) uses a similar approach in which the resulting effective width of the plate is located at the centroid of the longitudinally stiffened compression flange plate.

2) Unlike nonlongitudinally stiffened flange plates, longitudinally stiffened flange plates are unable to sustain large inelastic axial compressive strains beyond their maximum resistance. Therefore, the flexural resistance of box sections with a longitudinally stiffened compression flange is limited to the first yield of the compression flange in the effective cross-section.

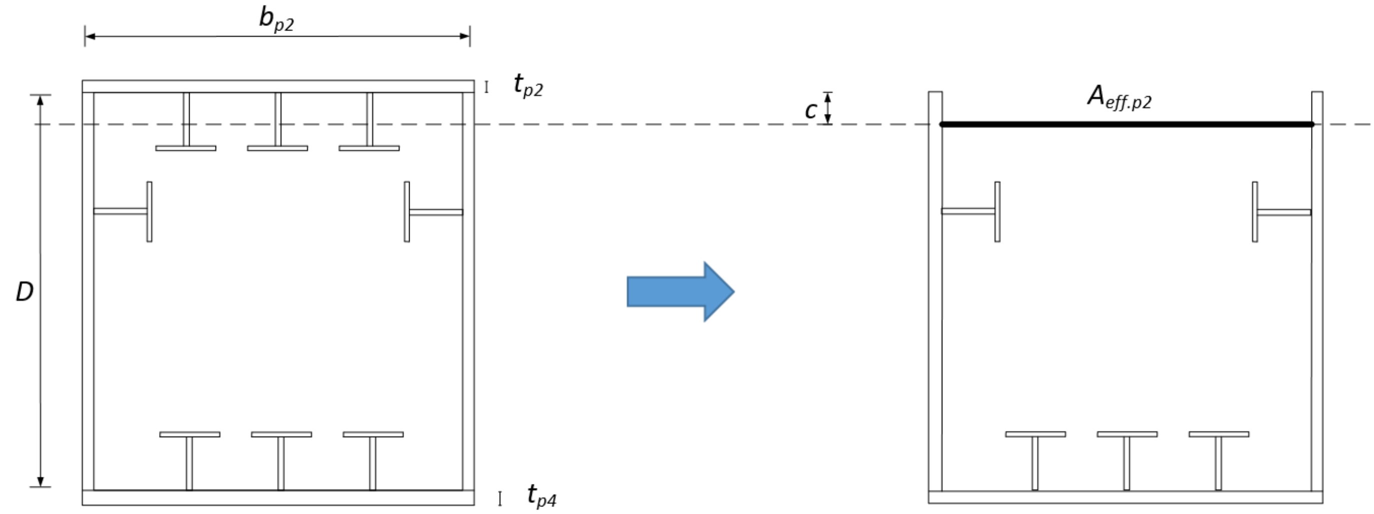

Figure 8: Effective box section considering the resistance of the stiffened compression flange

The nominal flexural resistance M_n of a welded box section with a longitudinally stiffened compression flange is calculated as follows:

If $L_b \le L_p$ then: $M_n = M_{cs}$ (41)

If $L_p < L_b \le L_r$ then: $M_n = C_b \left[M_{cs} - \left(M_{cs} - M_{pt2} \right) \left(\dfrac{L_b - L_p}{L_r - L_p} \right) \right] \le M_{cs}$ (42)

where:

M_{cs} = cross-section resistance, calculated as follows:

- For sections with $S_{xce} \le S_{xte}$,

  $M_{cs} = R_b R_h F_{yc} S_{xce}$ (43)

- For sections with $S_{xce} > S_{xte}$, it is recommended that the yield moment of the compression flange be determined directly, considering the early yielding of the section on the tension side of the neutral axis, and considering hybrid web, slender web and longitudinally stiffened compression flange effects as applicable. This calculation is explained in detail in Lokhande (2018). Unlike the case with $S_{xce} \le S_{xte}$, it is recommended that the AASHTO R_h expression should not be used to quantify the resistance of hybrid box sections for cases with $S_{xce} > S_{xte}$. Rather, the hybrid web effect should be incorporated into the calculation of the yield moment to the compression flange. Similarly, R_b cannot be used to address web bend buckling for cases with $S_{xce} > S_{xte}$ because R_b is derived such that the position of the neutral axis is dependent only on the loss of effectiveness of the webs due to bend buckling; it does not account for the shift in neutral axis because of the early yielding of the tension flange and the spread of yielding in the tension zone. In summary, for cases with $S_{xce} > S_{xte}$ a strain compatibility analysis should be used to account for web bend buckling, hybrid web effects and inelastic strength reserve corresponding to the spread of yielding in the tension zone, in the calculation of M_{cs}.

$$M_{pt2} = R_b F_{yr} S_{xce} \le M_{cs} \tag{44}$$

$$F_{yr} = 0.5F_{yc} \tag{45}$$

L_p is obtained by back-solving for L_b by taking the elastic lateral torsional buckling moment M_{cr} equal to $15M_{pe}$=$19.5M_{yce}$, assuming M_{pe}=$1.3M_{yce}$.

L_r is obtained by back-solving for L_b by taking the elastic lateral torsional buckling moment M_{cr} equal to $R_b F_{yr} S_{xce}$ and taking 30% of that length.

R_b is the web load-shedding factor explained in Subramanian and White (2017).

R_h is the hybrid factor. It should be calculated using AASHTO (2017) Eq. 6.10.1.10.1-1, but with A_{fn} taken as one-half of the total effective flange area $A_{eff.p2}/2$.

4.3 Salient features of the proposed methods

The proposed new methods encapsulate a significant advancement in the understanding of the behavior of longitudinally stiffened welded steel box-section members subjected to flexure and provide a more accurate and conceptually unified characterization of their resistance. The salient features of these methods are as follows:

1) They account for:

- The different failure modes of a longitudinally stiffened compression flange plate. The methods do this by more accurately quantifying the flange ultimate compressive resistance (discussed in Section 2), which is then used to determine an effective cross-section.
- Web bend buckling and the corresponding postbuckling resistance via the use of the R_b factor, or by using an effective cross-section as shown in Figs. 9 and 10, as applicable; this avoids the need to perform iterative or two-step calculations to obtain the effective cross-section.
- Lateral torsional buckling, including interaction with flange and web local buckling and postbuckling responses.

2) They cover all ranges of component plate slenderness.

3) They address singly as well as doubly-symmetric box sections. In bridges, it is common that fabricated boxes may be singly symmetric, and boxes with longitudinally stiffened compression flanges are inherently singly symmetric.

4) They address box sections with hybrid webs. It is possible for steel box-section members subjected to flexure to have webs with lower yield strength than that of the flanges.

5) They recognize the inelastic reserve strength corresponding to the spread of yielding in the tension zone for cases with $S_{xce} > S_{xte}$.

6) They recognize the inability of longitudinally stiffened flange plates to sustain large inelastic axial compressive strains beyond the peak load without a substantial reduction in their load carrying capacity, and therefore they limit the flexural resistance of box sections with a longitudinally stiffened compression flange to the first yield of the compression flange in the effective cross-section.

7) They eliminate the need to consider a separate tension flange yielding (TFY) limit state. For sections with $S_{xce} > S_{xte}$, the member response is addressed rigorously via the direct calculation of the yield moment to the compression flange, considering the early yielding of the section on the tension side of the neutral axis, and considering hybrid web, slender web and longitudinally stiffened compression flange effects as applicable.

8) The proposed methods are conceptually consistent with the method proposed by Lokhande and White (2017) for determining the flexural resistance of nonlongitudinally stiffened box-section members.

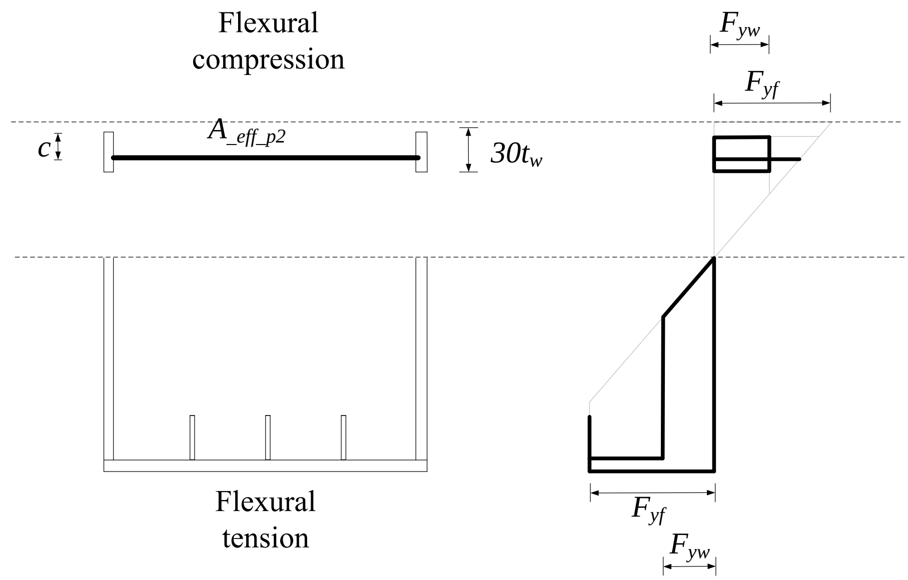

Figure 9: Stress distribution for box sections with unstiffened slender webs when $S_{xce} > S_{xte}$ (Lokhande 2018)

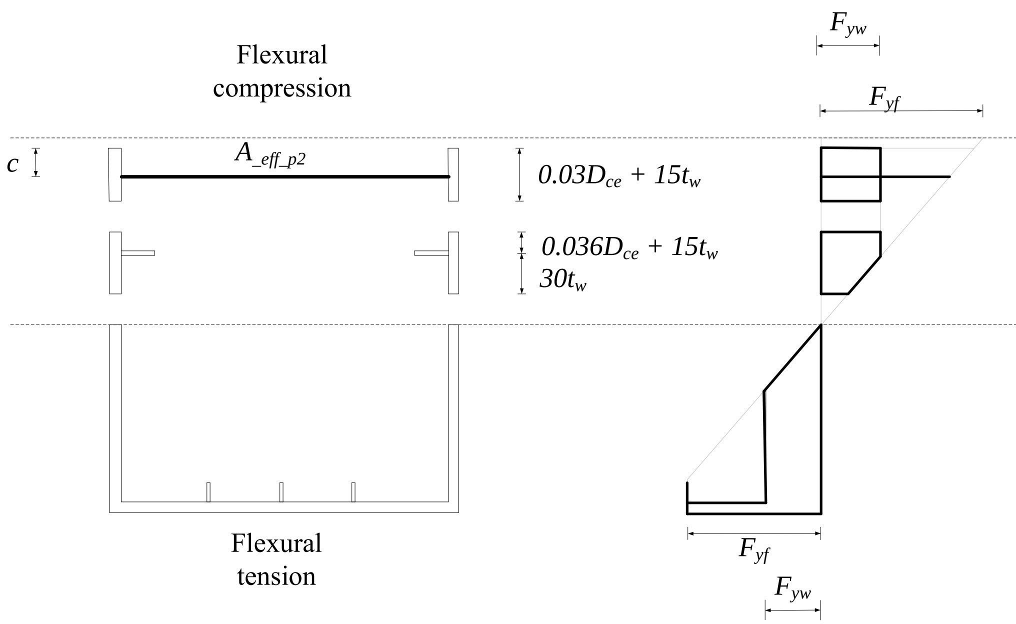

Figure 10: Stress distribution for box sections with longitudinally stiffened webs (with one longitudinal web stiffener in compression) and $\lambda_w > \lambda_{rw}$ when $S_{xce} > S_{xte}$ (Lokhande 2018)

4.4 Evaluation of the performance of the proposed methods

The performance of the proposed methods is evaluated using existing experimental data, and via a parametric study performed using FE simulations. The results of this study are discussed in detail in Lokhande (2018).

5. Summary and concluding remarks

This paper summarizes the conceptual and theoretical development of new methods for an improved characterization of the ultimate compressive resistance of longitudinally stiffened plates, and the flexural and axial compressive resistance of longitudinally stiffened welded box-section members. The methods described in the paper reflect a significant advancement in the understanding of the behavior of these member types. The predictions using these proposed methods correlate well with the results of parametric studies performed using finite element test simulations, and with data compiled from experimental tests.

Acknowledgements

This research is sponsored by the Federal Highway Administration. This financial support is gratefully acknowledged. The authors express special thanks to Mr. John Yadlosky (HDR Engineering Inc.), Mr. Anthony Ream (HDR Engineering Inc.), Dr. Francesco Russo (Michael Baker International), and Drs. Brian Kozy and Dayi Wang (FHWA Office of Bridges and Structures) for their valuable input. The opinions, findings, and conclusions expressed in this paper are those of the writers and do not necessarily reflect the views of the above mentioned individuals and organizations.

References

AASHTO (2017). "AASHTO LRFD Bridge Design Specifications." 8th Ed., American Association of State Highway and Transportation Officials, Washington DC.

AISI (2016). "North American Specification for the Design of Cold-Formed Steel Structural Members." American Iron and Steel Institute, Washington, DC.

CEN. (2005). "EN 1993-1-1. Eurocode 3: design of steel structures-Part 1-1: General rules and rules for buildings."

CEN. (2006). "EN 1993-1-5. Eurocode 3—design of steel structures-Part 1-5: Plated structural elements."

Chou, C. (2011). "Akashi Kaikyo Bridge." Retrieved from https://www.flickr.com/photos/chitaka/10109544695/

GSG (2013). "Lupu Bridge." Retrieved from https://www.globalsalesgrowth.com

King C.M. (2017). "A New Design Method for Longitudinally Stiffened Plates." Proceedings of the Annual Stability Conference, Structural Stability Research Council, San Antonio, TX, March.

Lokhande, A. and White, D.W. (2017). "Behavior and Design of NonComposite Nonlongitudinally Stiffened Welded Steel Box-Section Members." Proceedings of the Annual Stability Conference, Structural Stability Research Council, San Antonio, TX, March.

Lokhande, A. (2018). "Improved Characterization of the Flexural and Axial Compressive Resistance of Welded Steel Box Section Members." Ph.D. Dissertation, Georgia Institute of Technology (to appear).

Pekoz, T.B (1986). "Development of a Unified Approach to the Design of Cold-Formed Steel Members." Report SG-86-4, American Iron and Steel Institute, 1986.

Subramanian, L.P., and D.W. White. (2017). "Improved Strength Reduction Factors for Steel Girders with Longitudinally Stiffened Webs," Research Report, School of Civil and Environmental Engineering, Georgia Institute of Technology, Atlanta, GA, January.

White, D.W., A. Lokhande, C.M. King, M.A. Grubb, A. Ream., and F. Russo (2018). "LRFD Specifications for Noncomposite Steel Box Sections," Report to Federal Highway Administration, FHWA ID/IQ DTFH610-14-D-00049 (to appear).